Bollettino
Unione Matematica Italiana

Hitoshi Funagane, Shigeru Takata, Kazuo Aoki, Ko Kugimoto

Poiseuille Flow and Thermal Transpiration of a Rarefied Polyatomic Gas Through a Circular Tube with Applications to Microflows

Bollettino dell'Unione Matematica Italiana, Serie 9, Vol. **4** (2011), n.1, p. 19–46.

Unione Matematica Italiana

<http://www.bdim.eu/item?id=BUMI_2011_9_4_1_19_0>

Bollettino dell'Unione Matematica Italiana, Unione Matematica Italiana, 2011.

Bollettino U. M. I.
(9) **IV** (2011), 19-46

Poiseuille Flow and Thermal Transpiration of a Rarefied Polyatomic Gas Through a Circular Tube with Applications to Microflows

HITOSHI FUNAGANE - SHIGERU TAKATA - KAZUO AOKI - KO KUGIMOTO

To the memory of Carlo Cercignani

Abstract. – *As the first step, a rarefied polyatomic gas in a long and straight circular tube is considered, and the flow caused by a small uniform pressure gradient (Poiseuille flow) and the flow induced by a small uniform temperature gradient along the tube (thermal transpiration) are investigated, using the ellipsoidal statistical (ES) model of the Boltzmann equation for a polyatomic gas. It is shown that the solutions to these problems can be reduced to those based on the Bhatnagar-Gross-Krook (BGK) model for a monatomic gas. Numerical results of the velocity profiles, mass-flow rates, etc. for the Nitrogen gas, obtained by exploiting the existing database based on the BGK model, are shown. As the second step, a rarefied polyatomic gas in a long circular pipe is considered in the following situation: (i) the pressure and temperature variations along the pipe can be arbitrary and large; (ii) the length scale of variations is much longer than the radius of the pipe; (iii) the pipe may consist of circular tubes with different radii connected one after another. It is shown that, in this situation, the pressure distribution along the pipe is described by a macroscopic equation of diffusion type, with the diffusion coefficients consisting of the mass-flow rates of the Poiseuille flow and thermal transpiration, and an appropriate condition at the junction where the cross section changes suddenly. Then, the system is applied to a polyatomic gas flow through a single long pipe caused by a large pressure difference imposed at both ends and to a Knudsen compressor consisting of many alternately arranged thinner and thicker circular tubes.*

1. – Introduction.

The Poiseuille flow and thermal transpiration of a rarefied gas through a long tube are fundamental and classical problems in rarefied gas dynamics. The former is a flow driven by a small and uniform pressure gradient imposed along the tube, and the latter, which is peculiar to a rarefied gas, is a flow caused by a small and uniform temperature gradient along the tube. Since 1960's, these flows have been the subjects of many papers. From 1960's to 1980's, the linearized model Boltzmann equation, in particular, the Bhatnagar-Gross-Krook (BGK) model [7, 42], was used mainly both for theoretical and numerical analyses (see,

for example, Refs. [10, 11, 37, 23, 17] for the Poiseuille flow and Refs. [37, 23, 17, 22, 26] for the thermal transpiration). But after around 1990, accurate numerical analysis based on the linearized Boltzmann equation became possible (see, for example, Refs. [27] and [31]). The reader is referred to Ref. [30], which contains an extensive review of the works earlier than this reference. Mention should also be made of the recent development [31, 29], in particular, the mathematical study of the thermal transpiration [12].

The importance of these fundamental flows has rapidly been increased in connection with the recent progress of micro-mechanical systems because the small characteristic length leads the effect of rarefied gas to manifest itself even under atmospheric conditions. In practical applications, one encounters microscale systems with complex geometry, so that the direct application of kinetic theory, such as numerical simulations using the direct simulation Monte Carlo (DSMC) method, is computationally expensive and is not an efficient approach. Therefore, some heuristic macroscopic equations, which are intended to cover the transition regimes with non-small Knudsen numbers, have been proposed. The accurate numerical results for the Poiseuille flow and thermal transpiration provide a good standard for the assessment of these macroscopic equations.

On the other hand, in many microscale applications, gas-flow channels or pipes are very thin compared with their length. This property enables us to derive simple macroscopic equations systematically from kinetic theory without any ambiguity. Such an approach has been taken in some different applications (see, for example, Ref. [15] for a thin-gap slider bearing and Refs. [13] and [14] for plasma thrusters). Recently, macroscopic equations of the same type were constructed for the purpose of analyzing the property of the Knudsen compressor [2, 5], showing its applicability to gas separation [40], and investigating gas flows in a curved channel [4]. According to Ref. [5], the behavior of a gas in a thin pipe with an arbitrary but slowly-varying temperature distribution in the axial direction is described by a diffusion-type equation for any Knudsen number. The equation contains two functions, which correspond to the mass-flow rate of the Poiseuille flow and that of the thermal transpiration through the same pipe regarded as functions of the Knudsen number. Therefore, obtaining accurate data for the mass-flow rates of the Poiseuille flow and thermal transpiration for the whole range of the Knudsen number is essential for the application of the diffusion-type equation. Actually, in Ref. [5], the diffusion-type equation is applied to obtain the mass-flow rate and pressure distribution for the Knudsen pump, consisting of alternately arranged narrow and wide two-dimensional (2D) channels with a saw-tooth temperature distribution. In this application, use has been made of the database of the mass-flow rates of the Poiseuille flow and thermal transpiration between two parallel plates, constructed by the modified Knudsen-number expansion on the basis of the linearized BGK model [33].

Recently in Ref. [39], the macroscopic system of Ref. [5] was extended to a single polyatomic gas in the case of 2D channels, using the polyatomic version [1] of the Ellipsoidal Statistical (ES) model [18, 19] of the Boltzmann equation. In the present study, we carry out the same extension in the case of circular tubes and apply the resulting system to the Knudsen compressor consisting of circular pipes with different radii, as well as to the flow through a long circular tube driven by a large pressure difference at both ends. Since the extension is essentially the same as in the case of 2D channels, we will just summarize the result. However, since the Poiseuille flow and thermal transpiration in a circular tube, the mass-flow rates of which give the two coefficients occurring in the macroscopic system, are the problems of fundamental importance, we will spend more space to discuss these flows. In fact, as in the case of 2D channels, it turns out that the solution of the thermal transpiration through a circular tube based on the ES model for a polyatomic gas is identical with that based on the BGK model for a monatomic gas, and that the solution of the Poiseuille flow through a circular tube based on the ES model for a polyatomic gas is obtained by a simple conversion formula from that based on the BGK model for a monatomic gas.

The paper is organized as follows. In Sec. 2, we investigate Poiseuille flow and thermal transpiration of a rarefied polyatomic gas through an infinitely long straight tube with circular cross section on the basis of the linearized ES model for a polyatomic gas. After the formulation of the problems and some preliminary analysis (Secs. 2.1–2.3), we show that the problems can be reduced to the corresponding problems for the BGK model for a polyatomic gas (Sec. 2.4). Then, after some discussions of the properties of the mass-flow and heat-flow rates (Sec. 2.5), we show some numerical results (Sec. 2.6). In Sec. 3, we consider a rarefied polyatomic gas in a long circular tube with arbitrary and large temperature variation along the tube wall. The radius of the circular cross section may change discontinuously if the portion with a constant radius is long enough. The macroscopic equation of diffusion-type for such a tube, based on the ES model for a polyatomic gas, is summarized, together with the condition at the junction where the radius changes discontinuously. In Sec. 4, the macroscopic system is applied to a gas flow through a long circular pipe caused by a large pressure difference (Sec. 4.1) and to a Knudsen compressor composed of many long circular tubes (Sec. 4.2). Finally concluding remarks are given in Sec. 5.

2. – Poiseuille flow and thermal transpiration through a circular tube.

2.1 – *Problem, assumptions, and notations.*

Let us consider a rarefied polyatomic gas in an infinitely long and straight circular tube, and let δ be the number of degrees of freedom of a

gas molecule. We take the X_3 axis (of a rectangular coordinate system X_i) along the tube axis and let the radius of the tube be R_0. A uniform pressure gradient in the X_3 direction is imposed in the gas, and a uniform temperature gradient in the same direction is imposed along the tube wall. That is, the pressure p and the temperature of the tube wall T_w are expressed as $p_0(1 + aX_3/R_*)$ and $T_0(1 + \beta X_3/R_*)$, respectively, where R_* is a reference length (one may naturally let $R_* = R_0$, but we do not do so for later convenience). The fact that p is uniform in the cross section will be found later. We investigate the steady flow of the gas induced in the tube under the following assumptions.

(i) The behavior of the gas is described by the ES model [18, 19] of the Boltzmann equation for a polyatomic gas [1].

(ii) The gas molecules undergo diffuse reflection on the tube wall.

(iii) The imposed pressure gradient a and temperature gradient β are so small that the equation and boundary condition can be linearized around an equilibrium state at rest.

Before presenting the basic equations, we summarize other notations used in Sec. 2 (see also Appendix A). The symbol $\rho_0 = p_0/\mathcal{R}T_0$ denotes the density of the gas at $X_3 = 0$, $\mathcal{R}$ the gas constant per unit mass (the Boltzmann constant divided by the mass of a molecule), l_0 the mean free path of the gas molecules in the equilibrium state at rest at density ρ_0 and temperature T_0 (thus pressure p_0), and $\mathrm{Kn} = l_0/R_*$ the Knudsen number. Further, $x_i = X_i/R_*$, $(2\mathcal{R}T_0)^{1/2}\zeta_i$ is the molecular velocity, $\mathcal{R}T_0\mathcal{E}$ the energy related to the internal degree of freedom, $\Lambda_\delta \mathcal{E}^{\delta/2-1}(2\pi\mathcal{R}T_0)^{-3/2}(\mathcal{R}T_0)^{-1}\exp(-\zeta_i^2 - \mathcal{E})\rho_0(1 + \phi)$ the molecular velocity distribution function, Λ_δ the dimensionless constant defined by Eq. (48), $\rho_0(1 + \omega)$ the density of the gas, $T_0(1 + \tau)$ the temperature, $T_0(1 + \tau_{\mathrm{tr}})$ the temperature related to the translational energy, $T_0(1 + \tau_{\mathrm{int}})$ the temperature related to energy of the internal degree of freedom, $p_0(1 + P)$ the pressure, $(2\mathcal{R}T_0)^{1/2}u_i$ the flow velocity, $p_0(\delta_{ij} + P_{ij})$ the stress tensor, and $p_0(2\mathcal{R}T_0)^{1/2}Q_i$ the heat-flow vector. The quantities $|\phi|$, $|\omega|$, $|\tau|$, $|\tau_{\mathrm{tr}}|$, $|\tau_{\mathrm{int}}|$, $|P|$, $|u_i|$, $|P_{ij}|$, and $|Q_i|$ are assumed to be small. We introduce the cylindrical coordinate system (r, θ, x_3) in the dimensionless x_i space and denote by a_i and b_i the unit vector in the r direction and that in the θ direction, respectively. Then, we denote $\zeta_r = \zeta_i a_i$, $\zeta_\theta = \zeta_i b_i$, $u_r = u_i a_i$, $u_\theta = u_i b_i$, $Q_r = Q_i a_i$, $Q_\theta = Q_i b_i$, $P_{rr} = P_{ij}a_i a_j$, $P_{\theta\theta} = P_{ij}b_i b_j$, $P_{r\theta} = P_{\theta r} = P_{ij}a_i b_j$, $P_{r3} = P_{3r} = P_{i3}a_i$, $P_{\theta 3} = P_{3\theta} = P_{i3}b_i$. In addition, $\zeta = (\zeta_i^2)^{1/2} = (\zeta_r^2 + \zeta_\theta^2 + \zeta_3^2)^{1/2}$, and $E(\zeta, \mathcal{E}) = \pi^{-3/2}\Lambda_\delta \exp(-\zeta^2 - \mathcal{E})$. The summation convention $\left(\text{e.g., } \zeta_i a_i = \sum_{i=1}^{3} \zeta_i a_i\right)$ is used throughout the paper. We assume that the flow field is axisymmetric, i.e., ϕ in the cylindrical coordinate system does not depend on θ.

2.2 – *Basic equations.*

The linearized version of the ES model reads (see Appendix A for the original form of the model)

$$\zeta_r \frac{\partial \phi}{\partial r} + \frac{\zeta_\theta^2}{r}\frac{\partial \phi}{\partial \zeta_r} - \frac{\zeta_r \zeta_\theta}{r}\frac{\partial \phi}{\partial \zeta_\theta} + \zeta_3 \frac{\partial \phi}{\partial x_3} = \frac{2}{\sqrt{\pi}}\frac{1}{\mathrm{Kn}}(\phi_g - \phi), \tag{1}$$

with

$$\phi_g = \omega + 2\zeta_i u_i + \left(\zeta^2 - \frac{3}{2}\right)[(1-\eta)\tau_{\mathrm{tr}} + \eta\tau] + \left(\mathcal{E} - \frac{\delta}{2}\right)\tau_{\mathrm{rel}} + (1-\eta)\nu[P_{ij}\zeta_i\zeta_j - (\omega + \tau_{\mathrm{tr}})\zeta^2], \tag{2a}$$

$$\omega = \iint_0^\infty \mathcal{E}^{\delta/2-1}\phi E d\mathcal{E} d^3\zeta, \tag{2b}$$

$$u_i = \iint_0^\infty \zeta_i \mathcal{E}^{\delta/2-1}\phi E d\mathcal{E} d^3\zeta, \tag{2c}$$

$$\tau_{\mathrm{tr}} = \frac{2}{3}\iint_0^\infty \zeta^2 \mathcal{E}^{\delta/2-1}\phi E d\mathcal{E} d^3\zeta - \omega, \tag{2d}$$

$$\tau_{\mathrm{int}} = \frac{2}{\delta}\iint_0^\infty \mathcal{E}^{\delta/2}\phi E d\mathcal{E} d^3\zeta - \omega, \tag{2e}$$

$$\tau = \frac{3\tau_{\mathrm{tr}} + \delta\tau_{\mathrm{int}}}{3+\delta}, \tag{2f}$$

$$\tau_{\mathrm{rel}} = \eta\tau + (1-\eta)\tau_{\mathrm{int}}, \tag{2g}$$

$$P_{ij} = \iint_0^\infty 2\zeta_i\zeta_j \mathcal{E}^{\delta/2-1}\phi E d\mathcal{E} d^3\zeta, \tag{2h}$$

where $d^3\zeta = d\zeta_1 d\zeta_2 d\zeta_3 = d\zeta_r d\zeta_\theta d\zeta_3$, and ν and η are parameters to adjust the Prandtl number. The Knudsen number Kn is expressed as

$$\mathrm{Kn} = \frac{2}{\sqrt{\pi}}(1 - \nu + \eta\nu)\frac{(2\mathcal{R}T_0)^{1/2}\mu_0}{p_0 R_*}, \tag{3}$$

in terms of ν, η, and the viscosity μ_0 corresponding to the temperature T_0 [see Appendix A, Eq. (54a)]. In Eqs. (2b)-(2h) and in what follows, the domain of the integration with respect to ζ_i is its whole space, unless the contrary is stated.

The diffuse-reflection condition on the tube wall is written as

$$\phi = 2\sqrt{\pi}\int_{\zeta_r>0}\int_0^\infty \zeta_r \mathcal{E}^{\delta/2-1}\phi E d\mathcal{E} d^3\zeta + \left(\zeta^2 - 2 + \mathcal{E} - \frac{\delta}{2}\right)\beta x_3, \quad (r = R_0/R_*,\ \zeta_r < 0), \tag{4}$$

where $T_0(1+\beta x_3)$ is the temperature of the tube wall.

The linearized equation of state and the heat-flow vector are expressed as

$$P = \omega + \tau, \tag{5a}$$

$$Q_i = \iint_0^\infty \zeta_i(\zeta_j^2 + \mathcal{E})\mathcal{E}^{\delta/2-1}\phi E d\mathcal{E} d^3\zeta - \frac{5+\delta}{2}u_i. \tag{5b}$$

In addition, if we denote by $\rho_0(2\mathcal{R}T_0)^{1/2}\pi R_*^2 M$ the (dimensional) mass-flow rate (per unit time) through the tube, we have

$$M = 2\int_0^{R_0/R_*} u_3 r dr. \tag{6}$$

2.3 – *Similarity solutions.*

Let us introduce ζ_ρ and θ_ζ that express ζ_r and ζ_θ as

$$\zeta_r = \zeta_\rho \cos\,\theta_\zeta, \qquad \zeta_\theta = \zeta_\rho \sin\theta_\zeta, \tag{7}$$

(see Fig. 1) and transform the molecular velocity variables from $(\zeta_r, \zeta_\theta, \zeta_3)$ to $(\zeta_\rho, \theta_\zeta, \zeta_3)$. Note that $\zeta_\rho = (\zeta_r^2 + \zeta_\theta^2)^{1/2} = (\zeta_1^2 + \zeta_2^2)^{1/2}$ and $0 \le \zeta_\rho < \infty$, $-\pi < \theta_\zeta \le \pi$, and $-\infty < \zeta_3 < \infty$. Then, we seek the solution in the following form:

$$\phi = \left[a + \beta\left(\zeta_\rho^2 + \zeta_3^2 + \mathcal{E} - \frac{5+\delta}{2}\right)\right]x_3 + \zeta_3[a\,\Phi_P(r, \zeta_\rho, |\theta_\zeta|, \zeta_3^2, \mathcal{E}) + \beta\,\Phi_T(r, \zeta_\rho, |\theta_\zeta|, \zeta_3^2, \mathcal{E})]. \tag{8}$$

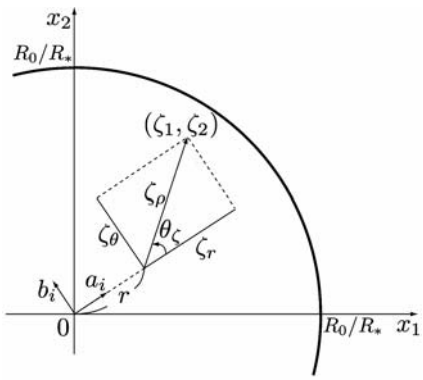

Fig. 1. – Coordinate system.

Actually, substitution of Eq. (8) into Eqs. (1) and (4) shows the consistency of Eq. (8) and leads to the following equation and boundary condition for Φ_J, where $J = P$ or T: The equation is

$$\zeta_\rho \cos\theta_\zeta \frac{\partial \Phi_J}{\partial r} - \frac{\zeta_\rho}{r}\sin\theta_\zeta \frac{\partial \Phi_J}{\partial \theta_\zeta} = \frac{2}{\sqrt{\pi}}\frac{1}{\mathrm{Kn}}[-\Phi_J + 2u_J + 2(1-\eta)\nu\zeta_\rho \cos\theta_\zeta \Pi_J] - I_J, \tag{9}$$

$$(0 \le r < R_0/R_*,\ 0 \le \zeta_\rho < \infty,\ 0 \le \theta_\zeta \le \pi,\ -\infty < \zeta_3 < \infty,\ 0 \le \mathcal{E} < \infty),$$

where

$$I_P = 1, \qquad I_T = \zeta_\rho^2 + \zeta_3^2 + \mathcal{E} - \frac{5+\delta}{2}, \tag{10a}$$

$$u_J = 2\int_{-\infty}^{\infty}\int_0^{\pi}\int_0^{\infty}\int_0^{\infty} \zeta_\rho \zeta_3^2 \mathcal{E}^{\delta/2-1}\Phi_J E d\mathcal{E} d\zeta_\rho d\theta_\zeta d\zeta_3, \tag{10b}$$

$$\Pi_J = 4\int_{-\infty}^{\infty}\int_0^{\pi}\int_0^{\infty}\int_0^{\infty} \zeta_\rho^2 \zeta_3^2 \cos\theta_\zeta \mathcal{E}^{\delta/2-1}\Phi_J E d\mathcal{E} d\zeta_\rho d\theta_\zeta d\zeta_3, \tag{10c}$$

$$E(\zeta, \mathcal{E}) = \Lambda_\delta \pi^{-3/2}\exp(-\zeta_\rho^2 - \zeta_3^2 - \mathcal{E}), \tag{10d}$$

and the boundary condition is

$$\Phi_J = 0, \tag{11}$$

$$(r = R_0/R_*,\ 0 \le \zeta_\rho < \infty,\ \pi/2 < \theta_\zeta \le \pi,\ -\infty < \zeta_3 < \infty, 0 \le \mathcal{E} < \infty).$$

In Eqs. (9)-(11), the range of θ_ζ has been reduced to $0 \le \theta_\zeta \le \pi$ by the use of the fact that Φ_J is an even function of θ_ζ.

The macroscopic quantities corresponding to Eq. (8) are obtained from Eqs. (2b)-(2h), (5a), and (5b) as follows.

$$\omega = (\alpha - \beta)x_3, \qquad P = \alpha x_3, \tag{12a}$$

$$u_r = u_\theta = 0, \qquad u_3 = \alpha u_P + \beta u_T, \tag{12b}$$

$$\tau_{\mathrm{tr}} = \tau_{\mathrm{int}} = \tau = \tau_{\mathrm{rel}} = \beta x_3, \tag{12c}$$

$$P_{rr} = P_{\theta\theta} = P_{33} = \alpha x_3, \qquad P_{r\theta} = P_{\theta 3} = 0, \qquad P_{r3} = \alpha\Pi_P + \beta\Pi_T, \tag{12d}$$

$$Q_r = Q_\theta = 0, \qquad Q_3 = \alpha Q_P + \beta Q_T, \tag{12e}$$

where u_J and Π_J are given in Eqs. (10b) and (10c), and Q_J by

$$Q_J = 2\int_{-\infty}^{\infty}\int_0^{\pi}\int_0^{\infty}\int_0^{\infty} \zeta_\rho \zeta_3^2 \left(\zeta_\rho^2 + \zeta_3^2 + \mathcal{E} - \frac{5+\delta}{2}\right)\mathcal{E}^{\delta/2-1}\Phi_J E d\mathcal{E} d\zeta_\rho d\theta_\zeta d\zeta_3. \tag{13}$$

That is, Eq. (8) indicates a flow in the axial direction with a uniform pressure and temperature gradients in the same direction. Note that the density, temperature, and pressure are independent of r. The solution Φ_P corresponds to the Poiseuille flow, and Φ_T to the thermal transpiration. Correspondingly, the dimensionless mass-flow rate [Eq. (6)] is expressed as

$$M = aM_P + \beta M_T, \tag{14a}$$

$$M_J = 2\int_0^{R_0/R_*} u_J r dr. \tag{14b}$$

If we multiply Eq. (9) by $\zeta_\rho \zeta_3^2 \mathcal{E}^{\delta/2-1} E$ and integrate it with respect to $\mathcal{E}$, ζ_ρ, θ_ζ, and ζ_3 over the domain $0<\mathcal{E}<\infty$, $0<\zeta_\rho<\infty$, $0<\theta_\zeta<\pi$, and $-\infty<\zeta_3<\infty$, we have

$$\frac{d\Pi_J}{dr} + \frac{\Pi_J}{r} = \begin{cases} -1 & (J=P), \\ 0 & (J=T). \end{cases} \tag{15}$$

Since Π_J should be finite at $r=0$, it is obtained as

$$\Pi_P = -\frac{r}{2}, \qquad \Pi_T = 0. \tag{16}$$

Equation (16) simplifies Eq. (9) further.

2.4 – *Further transformation and reduction to the BGK model.*

The system, Eqs. (9) [with Eq. (16)] and (11), can be simplified further by multiplying by $(2/\sqrt{\pi})\Lambda_\delta \mathcal{E}^{\delta/2-1}\zeta_3^2 \exp(-\mathcal{E}-\zeta_3^2)$ and integrating with respect to $\mathcal{E}$ from 0 to ∞ and ζ_3 from $-\infty$ to ∞. The resulting system is as follows: The equation is

$$\begin{aligned} &\zeta_\rho \cos\theta_\zeta \frac{\partial \Psi_J}{\partial r} - \frac{\zeta_\rho}{r}\sin\theta_\zeta \frac{\partial \Psi_J}{\partial \theta_\zeta} \\ &\quad = \frac{2}{\sqrt{\pi}}\frac{1}{\mathrm{Kn}}\left[-\Psi_J + 2u_J[\Psi_J] + 2\left(1-\frac{1}{\mathrm{Pr}}\right)\zeta_\rho \cos\theta_\zeta \Pi_J\right] - \tilde{I}_J, \\ &\qquad\qquad (0 \le r < R_0/R_*,\ 0 \le \zeta_\rho < \infty,\ 0 \le \theta_\zeta \le \pi), \end{aligned} \tag{17}$$

where

$$u_J[\Psi_J] = \frac{1}{\pi}\int_0^\pi \int_0^\infty \zeta_\rho \Psi_J \exp(-\zeta_\rho^2) d\zeta_\rho d\theta_\zeta, \tag{18a}$$

$$\Pi_P = -\frac{r}{2}, \qquad \Pi_T = 0, \tag{18b}$$

$$\tilde{I}_P = 1, \qquad \tilde{I}_T = \zeta_\rho^2 - 1, \tag{18c}$$

and the boundary condition is

$$\Psi_J = 0 \qquad (r = R_0/R_*,\ 0 \le \zeta_\rho < \infty,\ \ \pi/2 < \theta_\zeta \le \pi). \tag{19}$$

Here, Ψ_J is defined by

$$\Psi_J = \frac{2}{\sqrt{\pi}} \Lambda_\delta \int_{-\infty}^{\infty} \int_{0}^{\infty} \mathcal{E}^{\delta/2-1} \zeta_3^2 \Phi_J \exp(-\mathcal{E} - \zeta_3^2) d\mathcal{E} d\zeta_3. \tag{20}$$

Once the solution Ψ_J (and thus u_J) of Eqs. (17)-(19) is obtained, one can reconstruct the original Φ_J by solving Eq. (9), which reduces to a partial differential equation for Φ_J, under the boundary condition (11). Therefore, any macroscopic quantity, such as Q_J in Eq. (13), can be obtained. For convenience of discussion below, we rewrite the mass-flow rates M_J [Eq. (14)] in the following form:

$$M_J[\Psi_J] = 2 \int_0^{R_0/R_*} u_J[\Psi_J] r dr. \tag{21}$$

Here, we note that Eqs. (17)-(19) are of the same form as the corresponding equations and boundary conditions for the cylindrical Poiseuille flow and thermal transpiration based on the ES model for a monatomic gas [6]. The difference between monatomic and polyatomic gases arises only in the different values of Pr. Furthermore, Eqs. (17)-(19) with $J = T$, which do not contain Pr, are the same as the corresponding equation and boundary condition for the thermal transpiration based on the BGK model. As for the cylindrical Poiseuille flow, although Eqs. (17)-(19) with $J = P$ are different from the corresponding equation and boundary condition based on the BGK model, we can reduce the solution of the former to that of the latter by a simple conversion, as in the case of the plane Poiseuille flow. Let us put

$$\Psi_P = \Psi'_P - \frac{1}{\sqrt{\pi}} \frac{1}{\mathrm{Kn}} \left(1 - \frac{1}{\mathrm{Pr}}\right) \left[r^2 - \left(\frac{R_0}{R_*}\right)^2\right]. \tag{22}$$

Then, it follows from Eqs. (17)-(19) with $J = P$ that Ψ'_P satisfies

$$\zeta_\rho \cos\theta_\zeta \frac{\partial \Psi'_P}{\partial r} - \frac{\zeta_\rho}{r} \sin\theta_\zeta \frac{\partial \Psi'_P}{\partial \theta_\zeta} = \frac{2}{\sqrt{\pi}} \frac{1}{\mathrm{Kn}} \left(-\Psi'_P + 2u_P[\Psi'_P]\right) - 1, \tag{23a}$$

$$\Psi'_P = 0 \qquad (r = R_0/R_*,\ \pi/2 < \theta_\zeta \le \pi), \tag{23b}$$

which are identical with the corresponding equation and boundary condition for the cylindrical Poiseuille flow based on the BGK model. To summarize these facts, we obtain the following relations for the solutions, flow velocities, and mass-flow rates:

$$\Psi_P = \Psi_P^{\mathrm{BGK}} - \frac{1}{\sqrt{\pi}}\frac{1}{\mathrm{Kn}}\left(1-\frac{1}{\mathrm{Pr}}\right)\left[r^2 - \left(\frac{R_0}{R_*}\right)^2\right], \tag{24a}$$

$$u_P[\Psi_P] = u_P[\Psi_P^{\mathrm{BGK}}] - \frac{1}{2\sqrt{\pi}}\frac{1}{\mathrm{Kn}}\left(1-\frac{1}{\mathrm{Pr}}\right)\left[r^2 - \left(\frac{R_0}{R_*}\right)^2\right], \tag{24b}$$

$$u_T[\Psi_T] = u_T[\Psi_T^{\mathrm{BGK}}], \tag{24c}$$

$$M_P[\Psi_P] = M_P[\Psi_P^{\mathrm{BGK}}] + \frac{1}{4\sqrt{\pi}}\frac{1}{\mathrm{Kn}}\left(1-\frac{1}{\mathrm{Pr}}\right)\left(\frac{R_0}{R_*}\right)^4, \tag{24d}$$

$$M_T[\Psi_T] = M_T[\Psi_T^{\mathrm{BGK}}], \tag{24e}$$

where Ψ_P^{BGK} and Ψ_T^{BGK} are the solutions corresponding to Ψ_P and Ψ_T for the BGK model. As mentioned in Sec. 1, the database of $u_P[\Psi_P^{\mathrm{BGK}}]$, $u_T[\Psi_T^{\mathrm{BGK}}]$, $M_P[\Psi_P^{\mathrm{BGK}}]$, and $M_T[\Psi_T^{\mathrm{BGK}}]$, the original version of which was built by Sone and Itakura [33], has been constructed by Sone, Itakura, and Handa. From this, one can obtain an accurate values of these quantities instantaneously for an arbitrary Knudsen number. The database is available from the present authors (the software package can be downloaded from the webpage http://www.mfd.me.kyoto-u.ac.jp/Sone/database-e.html). Therefore, we do not need to carry out new computations to obtain u_P, u_T, M_P, and M_T for the ES model for a polyatomic gas. It should be noted that the conversion formula for the mass-flow rate of the Poiseuille flow between the ES model for a monatomic gas and the BGK model, corresponding to Eq. (24d), is given in Ref. [8].

2.5 – *Mass-flow and heat-flow rates.*

If we denote by $\mathcal{M}$ the total mass-flow rate in the X_3 direction per unit time, then it follows from Eqs. (6) and (14) that

$$\mathcal{M} = \pi\rho_0(2\mathcal{R}T_0)^{1/2}R_*^2\left[M_P(\mathrm{Kn};\, R_0/R_*)\,\frac{R_*}{p_0}\frac{dp}{dX_3} + M_T(\mathrm{Kn};\, R_0/R_*)\,\frac{R_*}{T_0}\frac{dT_w}{dX_3}\right], \tag{25}$$

where

$$M_J(\mathrm{Kn};\, R_0/R_*) = 2\int_0^{R_0/R_*} u_J\, r dr, \qquad (J = P,\ T). \tag{26}$$

Here, the fact that M_J depends on Kn and R_0/R_* is shown explicitly as arguments.

Now we take the radius of the circular tube R_0 as the reference length R_* and denote the corresponding Kn by Kn_0, i.e., $\mathrm{Kn} = (R_0/R_*)\,\mathrm{Kn}_0$. Then Eq. (25) becomes

$$\mathcal{M} = \pi\rho_0(2\mathcal{R}T_0)^{1/2}R_0^2\left[M_P(\mathrm{Kn}_0;\,1)\,\frac{R_0}{p_0}\,\frac{dp}{dX_3} + M_T(\mathrm{Kn}_0;\,1)\,\frac{R_0}{T_0}\,\frac{dT_w}{dX_3}\right]. \tag{27}$$

Since Eqs. (25) and (27) express the same quantity, we have the following relation:

$$M_J(\mathrm{Kn};\,R_0/R_*) = (R_0/R_*)^3 M_J(\mathrm{Kn}_0;\,1). \tag{28}$$

Similarly, from the solution Φ_J (or Q_J), we can compute the heat-flow rate through the tube. Let $\mathcal{H}$ be the total heat-flow rate in the X_3 direction per unit time. Then we have

$$\mathcal{H} = \pi p_0(2\mathcal{R}T_0)^{1/2}R_*^2\left[H_P(\mathrm{Kn};\,R_0/R_*)\,\frac{R_*}{p_0}\,\frac{dp}{dX_3} + H_T(\mathrm{Kn};\,R_0/R_*)\,\frac{R_*}{T_0}\,\frac{dT_w}{dX_3}\right], \tag{29}$$

where

$$H_J(\mathrm{Kn};\,R_0/R_*) = 2\int_0^{R_0/R_*} Q_J\,r\,dr, \qquad (J = P,\ T), \tag{30}$$

and it satisfies the following relation:

$$H_J(\mathrm{Kn};\,R_0/R_*) = (R_0/R_*)^3 H_J(\mathrm{Kn}_0;\,1). \tag{31}$$

2.6 – *Numerical results.*

In this Sec. 2.6, we show the profiles of the velocity and heat flow and mass-flow rates for the Poiseuille flow and thermal transpiration obtained with the help of Eq. (24). The basic equation (1) contains the set of parameters (ν, η, δ) to characterize the polyatomic gas under consideration. In place of this set, we may also use another set (Pr, μ_b/μ, δ) because of relations (51c), (51d), and (52). Here, we consider the nitrogen gas (N_2; $\delta = 2$), for which experimental data for Pr and μ_b/μ are available (Pr = 0.718 [25] and $\mu_b/\mu = 0.731$ [28]). We set the values of ν and η in such a way that the resulting Pr and μ_b/μ are close to the above experimental values, that is, $\nu = -0.50$ and $\eta = 0.46$, which lead to Pr = 0.787 and $\mu_b/\mu = 0.722$. We also set $R_* = R_0$ and assume A_c in Eq. (47) to be constant.

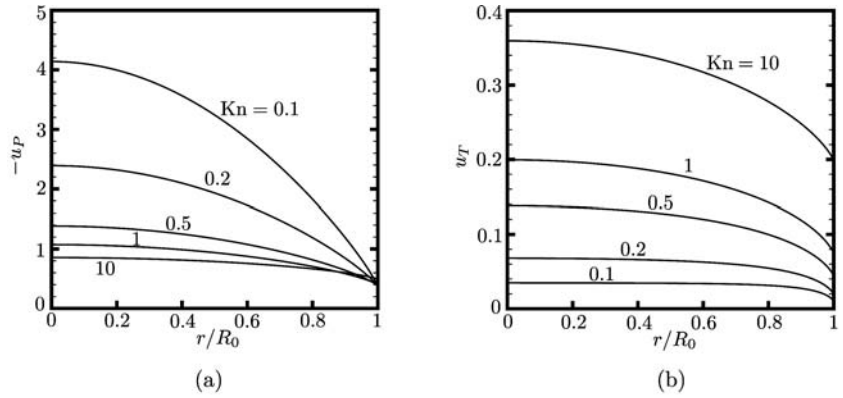

Fig. 2. – Profiles of the flow velocities for the Poiseuille flow and thermal transpiration through a circular tube. (a) Dimensionless flow velocity u_P for the Poiseuille flow. (b) Dimensionless flow velocity u_T for the thermal transpiration.

Figures 2(a) and 2(b) show the velocity profile for the Poiseuille flow u_P and that for the thermal transpiration u_T for various values of Kn [cf. Eq. (12b)]. Figures 3(a) and 3(b) show the corresponding profiles of the heat-flow vectors Q_P and Q_T [cf. Eq. (12e)]. Tables 1 and 2 show the mass-flow rates M_P and M_T versus Kn, respectively. In Table 1, the result for a monatomic gas ($\mathrm{Pr} = 2/3$) is also shown for comparison (M_T in Table 2 does not depend on the value of Pr and is the same as that for the BGK model).

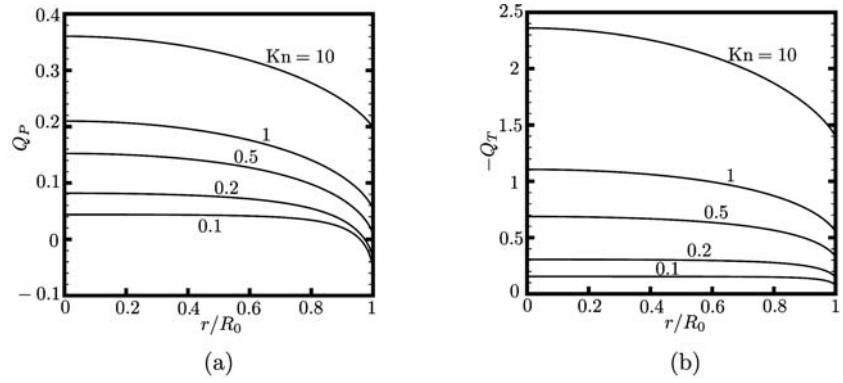

Fig. 3. – Profiles of the heat-flow vectors for the Poiseuille flow and thermal transpiration through a circular tube. (a) Dimensionless heat-flow vector Q_P for the Poiseuille flow. (b) Dimensionless heat-flow vector Q_T for the thermal transpiration.

TABLE 1. – Dimensionless mass-flow rate M_P for the Poiseuille flow.

Kn	$-M_P\|_{\mathrm{Pr}=2/3}$	$-M_P\|_{\mathrm{Pr}=0.787}$
10^{-2}	0.2167(2)*	0.1843(2)
2×10^{-2}	0.1109(2)	0.9474(1)
3×10^{-2}	0.7567(1)	0.6489(1)
4×10^{-2}	0.5807(1)	0.4998(1)
6×10^{-2}	0.4048(1)	0.3509(1)
8×10^{-2}	0.3170(1)	0.2766(1)
10^{-1}	0.2645(1)	0.2322(1)
2×10^{-1}	0.1604(1)	0.1442(1)
3×10^{-1}	0.1263(1)	0.1155(1)
4×10^{-1}	0.1096(1)	0.1015(1)
6×10^{-1}	0.9336(0)	0.8797
8×10^{-1}	0.8558(0)	0.8154
1	0.8112	0.7788
5	0.7037	0.6972
10^1	0.7068	0.7035
10^2	0.7377	0.7373
10^3	0.7496	0.7495
10^4	0.7519	0.7519

* Read as 0.2167×10^2.

TABLE 2. – Dimensionless mass-flow rate M_T for the thermal transpiration.

Kn	M_T
10^{-2}	0.3364(−2)*
2×10^{-2}	0.6665(−2)
3×10^{-2}	0.9903(−2)
4×10^{-2}	0.1308(−1)
6×10^{-2}	0.1923(−1)
8×10^{-2}	0.2514(−1)
10^{-1}	0.3079(−1)
2×10^{-1}	0.5558(−1)
3×10^{-1}	0.7555(−1)
4×10^{-1}	0.9197(−1)
6×10^{-1}	0.1176
8×10^{-1}	0.1370
1	0.1524
5	0.2579
10^1	0.2934
10^2	0.3573
10^3	0.3730
10^4	0.3757

* Read as 0.3364×10^{-2}.

3. – Diffusion-type system.

In this section, we consider a rarefied polyatomic gas in a straight pipe composed of long circular tubes connected longitudinally. The radius of each tube is different each other, as shown in Fig. 4. Therefore, the cross section of the pipe changes suddenly at the junctions of the tubes. We assume the following:

(i) The behavior of the gas is described by the ES model for a polyatomic gas.

(ii) The gas molecules undergo diffuse reflection on the pipe wall (including the walls at the junctions).

(iii) The length of each circular tube is much longer than its diameter.

(iv) The temperature of the pipe wall is uniform at each cross section (and at each junction). The distribution of the wall temperature along the pipe axis is arbitrary but continuous (its derivative may be discontinuous at the junctions), and its variation may be large. However, the length scale of its variation is much longer than the diameters of the tubes.

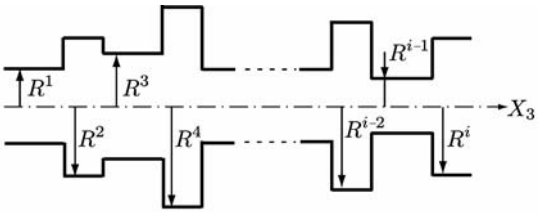

Fig. 4. – Schematic of the straight pipe.

In this situation, one can derive, by a systematic asymptotic analysis of the kinetic system, a macroscopic system consisting of a diffusion-type equation in each tube and a connection condition at each junction that describes the (slow) time evolution of the distribution of the pressure (or density) of the gas along the pipe axis. In Ref. [5], such a system was derived for a single and monatomic gas for tubes with arbitrary (not necessarily circular) cross sections on the basis of the Boltzmann equation and a general form of the boundary condition. Here, we repeat the same analysis for the ES model for a polyatomic gas with the diffuse reflection condition and for circular tubes. Since analysis is basically the same as that in Refs. [40] and [5], we only summarize the result.

We assume that the axis of the pipe is set along the X_3 axis. Let t be the time variable, $T_w(X_3)$ the temperature of the pipe wall, T the temperature of the gas, ρ the density of the gas, $p = \mathcal{R}\rho T$ the pressure of the gas, and $\mathcal{M}$ is the mass-flow rate across the pipe in the X_3 direction per unit time. Let L_* denote the reference length in the axial direction (a typical length of the tubes, the length scale of variation of the temperature, etc.), R_* ($\ll L_*$) the reference length in the radial direction (a typical radius of the tubes), T_* the reference temperature, ρ_* the reference density, $p_* = \mathcal{R}\rho_* T_*$ the reference pressure, l_* the reference mean

free path of the gas molecules defined as $l_* = (2/\sqrt{\pi})(2\mathcal{R}T_*)^{1/2}/A_c(T_*)\rho_*$ (see Appendix A), and $K_* = l_*/R_*$ the reference Knudsen number. Furthermore, we introduce the following dimensionless quantities:

$$\hat{t} = t\,[L_*^2/(2\mathcal{R}T_*)^{1/2}R_*]^{-1}, \quad z = X_3/L_* \tag{32a}$$

$$\hat{T}_w = T_w/T_*, \quad \hat{\rho} = \rho/\rho_*, \quad \hat{T} = T/T_*, \quad \hat{p} = p/p_* \ (= \hat{\rho}\hat{T}), \tag{32b}$$

$$M = \mathcal{M}/\pi\rho_*(2\mathcal{R}T_*)^{1/2}R_*^2. \tag{32c}$$

The quantities $\hat{\rho}$, $\hat{T}$, $\hat{p}$, and M are expanded in terms of a small parameter $\varepsilon = R_*/L_*$ as

$$\hat{\rho} = \hat{\rho}_{(0)} + \hat{\rho}_{(1)}\varepsilon + \cdots, \tag{33a}$$

$$\hat{T} = \hat{T}_{(0)} + \hat{T}_{(1)}\varepsilon + \cdots, \tag{33b}$$

$$\hat{p} = \hat{p}_{(0)} + \hat{p}_{(1)}\varepsilon + \cdots, \tag{33c}$$

$$M = M_{(1)}\varepsilon + \cdots, \tag{33d}$$

and $\hat{\rho}_{(0)}$, $\hat{T}_{(0)}$, $\hat{p}_{(0)}$, and $M_{(1)}$ are found to be the functions of $\hat{t}$ and z (i.e., they do not depend on the radial coordinate). In addition, $\hat{T}_{(0)}(\hat{t}, z) = \hat{T}_w(z)$ holds, so that $\hat{p}_{(0)}(\hat{t}, z) = \hat{\rho}_{(0)}(\hat{t}, z)\hat{T}_w(z)$.

Let us consider the ith tube and denote $\hat{p}_{(0)}$ and $M_{(1)}$ there by $\hat{p}^i_{(0)}$ and $M^i_{(1)}$, respectively. Let R^i and $\hat{R}^i = R^i/R_*$ be the dimensional and dimensionless radii of the ith tube, respectively. Then, $\hat{p}^i_{(0)}$ is governed, through $M^i_{(1)}$, by the following equation:

$$\frac{\partial \hat{p}^i_{(0)}}{\partial \hat{t}} + \frac{\hat{T}_w}{(\hat{R}^i)^2}\frac{\partial M^i_{(1)}}{\partial z} = 0, \tag{34a}$$

$$M^i_{(1)} = \frac{\hat{p}^i_{(0)}}{\hat{T}_w^{1/2}}\left[M^i_P(K^i)\frac{\partial \ln \hat{p}^i_{(0)}}{\partial z} + M^i_T(K^i)\frac{d \ln \hat{T}_w}{dz}\right], \tag{34b}$$

where

$$K^i = \frac{K_*\hat{T}_w^{3/2}}{\hat{A}_c(\hat{T}_w)\hat{p}^i_{(0)}}, \tag{35}$$

and we have assumed that $A_c(T)$ in Eq. (47) can be written as

$$A_c(T) = A_c(T_*\hat{T}) = A_c(T_*)\hat{A}_c(\hat{T}). \tag{36}$$

(If $A_c = \text{const} \times T^m$, then $\hat{A}_c = \hat{T}^m$.) Here, $M^i_P(K^i)$ and $M^i_T(K^i)$ correspond to the dimensionless mass-flow rate of the Poiseuille flow and that of the thermal transpiration through an infinitely long circular tube with radius R^i. More precisely, they are related to $M_P(\text{Kn}; R_0/R_*)$ and $M_T(\text{Kn}; R_0/R_*)$ in Sec. 2.5 [cf.

Eqs. (26) and (28)] as

$$M_J^i(K^i) = M_J(K^i;\, \hat{R}^i) = (\hat{R}^i)^3 M_J(K^i/\hat{R}^i;\, 1) \qquad (J = P,\ T). \tag{37}$$

At the junction of the ith tube with the neighboring $(i+1)$th tube, the following connection condition has to be satisfied:

$$\hat{p}^i_{(0)} = \hat{p}^{i+1}_{(0)}, \qquad M^i_{(1)} = M^{i+1}_{(1)}. \tag{38}$$

Equations (34) and (38) are to be supplemented by an appropriate initial condition and end conditions (see Sec. 4.2). Once the solution of this system is found, the dimensional pressure p^i and the dimensional mass-flow rate $\mathcal{M}^i$ in the ith tube are given, respectively, by [cf. Eqs. (32) and (33)]

$$p^i = p_*[\hat{p}^i_{(0)} + O(\varepsilon)], \tag{39a}$$

$$\mathcal{M}^i = \pi\rho_*(2\mathcal{R}T_*)^{1/2} R_*^2 [M^i_{(1)}\varepsilon + O(\varepsilon^2)]. \tag{39b}$$

4. – Applications of diffusion-type system.

In this section, we apply the diffusion-type equation with the connection condition summarized in Sec. 3 to two problems. As in Sec. 2.6, we consider the nitrogen gas and let $\nu = -0.50$ and $\eta = 0.46$, which lead to $\mathrm{Pr} = 0.787$ and $\mu_b/\mu = 0.722$. We also assume A_c in Eq. (47) to be constant (thus $\hat{A}_c = 1$).

4.1 – *Flow caused by a large pressure difference.*

We first consider a single long circular tube of radius R_0 and length L kept at a uniform temperature T_0 and set in the interval $0 \le X_3 \le L$. Let both ends of the tube be open, and the pressure at $X_3 = 0$ and that at $X_3 = L$ be kept at p_0 and p_1, respectively. We investigate the steady flow of the gas through the tube.

Let us take p_0, T_0, R_0, and L as the reference quantities p_*, T_*, R_*, and L_*, respectively. Then, $\hat{T}_w = 1$, and K_* is the Knudsen number based on R_0, p_0, and T_0. In addition, we omit the superscript i in Eqs. (34), (35), (37), and (39). Then, the end conditions become

$$\hat{p}_{(0)} = 1 \ \ (\text{at}\ \ z = 0), \qquad \hat{p}_{(0)} = p_1/p_0 \ \ (\text{at}\ \ z = 1). \tag{40}$$

We solve Eq. (34) with end conditions (40) and an appropriate initial condition, e.g., $\hat{p}_{(0)} = 1$ at $\hat{t} = 0$ for $0 < z < 1$, and obtain the steady flow as the long-time limit of the solution. In the final steady state, since $\partial\hat{p}_{(0)}/\partial\hat{t} = 0$ holds, we have $M_{(1)} \equiv M_f = \text{const.}$, and the mass-flow rate $\mathcal{M}$ is given by [cf. Eq. (39b)]

$$\mathcal{M} = \pi\rho_0(2\mathcal{R}T_0)^{1/2} R_0^2\, [M_f\varepsilon + O(\varepsilon^2)], \tag{41}$$

where $\rho_0 = p_0/\mathcal{R}T_0$ and $\varepsilon = R_0/L$. Since the numerical solution method is straightforward, we show only the result of analysis.

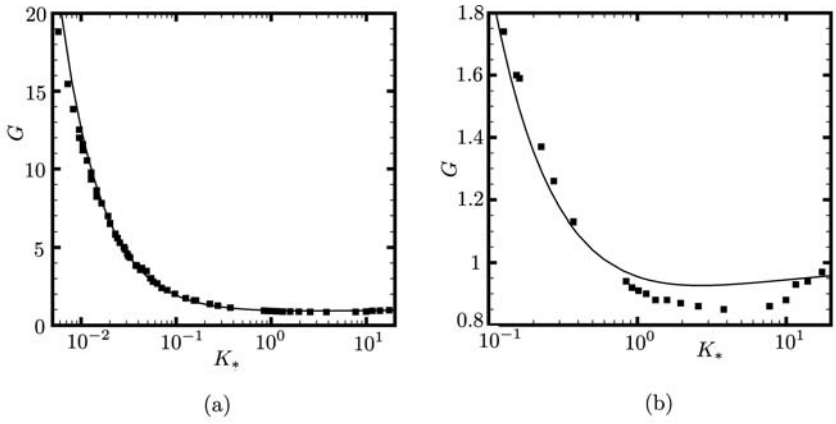

Fig. 5. – Reduced mass-flow rate G [$\equiv (3\sqrt{\pi}/4)M_f$] vs K_* for N_2 gas in the case of $p_1/p_0 = 10^{-2}$. (a) $0.005 \leq K_* \leq 20$, (b) magnified figure for $0.1 \leq K_* \leq 20$. The solid line indicates the numerical result ($\mathrm{Pr} = 0.787$ and $\mu_b/\mu = 0.722$), and the black square indicates the experimental result taken from Ref. [24].

Figure 5 shows the reduced mass-flow rate G versus K_* for $p_1/p_0 = 10^{-2}$. Here, $G = \mathcal{M}/\mathcal{M}_{\mathrm{FM}} = (3\sqrt{\pi}/4)[1 - (p_1/p_0)]^{-1}M_f \approx (3\sqrt{\pi}/4)M_f$ [with the term of $O(\varepsilon^2)$ neglected in Eq. (41)], and $\mathcal{M}_{\mathrm{FM}}$ is the mass-flow rate for the free-molecular flow, i.e., $\mathcal{M}_{\mathrm{FM}} = (4\sqrt{\pi}/3)R_0^3[(p_0 - p_1)/L](2/\mathcal{R}T_0)^{1/2}$. In the figure, the solid line indicates the numerical result for N_2 gas ($\mathrm{Pr} = 0.787$ and $\mu_b/\mu = 0.722$), and the black square indicates the experimental result taken from Ref. [24], where the experiment of the same problem is carried out with the nitrogen gas, using a bundle of huge number of tiny circular tubes, under the condition that $p_1/p_0 \approx 0$ and $\varepsilon = 1/2727$. Figure 5(a) shows the results for $0.005 \leq K_* \leq 20$ and Fig. 5(b) is the magnified figure for $0.1 \leq K_* \leq 20$. The pressure ratio p_1/p_0 in the present example might be too small to apply the diffusion-type system with confidence. Nevertheless, the numerical and experimental results show good agreement on the whole, except for the difference of 10% to 15% in the range $0.5 \leq K_* \leq 8$.

In Fig. 5, the experimental data are plotted after a suitable conversion of the Knudsen number, which is explained in the following. In Ref. [24], the mean free path l_0 is defined by $l_0 = kT_0/\sqrt{2}\pi d^2 p_0$ (with k the Boltzmann constant), assuming that an N_2 molecule is a hard sphere with effective diameter d. Therefore, it is expressed in terms of the viscosity μ_0 at temperature T_0 and pressure p_0 as $l_0 = (2/\sqrt{\pi})(\mu_0/\gamma_1)(2\mathcal{R}T_0)^{1/2}/p_0$ where $\gamma_1 = 1.270042$ [32]. On the other hand, from Eqs. (51c) and (54a), our l_0 is given by $l_0 = (2/\sqrt{\pi})(\mu_0/\mathrm{Pr})(2\mathcal{R}T_0)^{1/2}/p_0$. If we assume that the viscosity μ_0 is a common quantity and eliminate it from the two expressions for l_0, we obtain a conversion formula for l_0 between our nu-

merical result and experimental data in Ref. [24]. That is, in terms of the Knudsen number, we have $K_* = (\gamma_1/\mathrm{Pr})\,\mathrm{Kn}_i = 1.613777\,\mathrm{Kn}_i$, where Kn_i is the Knudsen number (at temperature T_0 and pressure p_0) in Ref. [24]. For instance, the measured value for $\mathrm{Kn}_i = 1$ is plotted at $K_* = 1.613777$ in Fig. 5.

4.2 – *Knudsen compressor.*

The Knudsen compressor [20, 21] is a non-mechanical device that produces a one-way gas flow with a pumping effect using the imbalance of the thermal transpiration caused by periodic temperature distribution and periodic structure of the device. It has been attracting attention as a microscale flow controller (e.g., Refs. [36, 41, 34, 35, 16]) and gas separator (e.g., Ref. [40]) without any moving parts, and its variants (e.g., Refs. [38] and [3]) have been proposed. A typical Knudsen pump is a long pipe with a periodic structure consisting of alternately arranged narrow and wide pipes. The temperature of the pipe is also periodic with the same period as the structure, such as a saw-tooth distribution increasing in the narrow segments and decreasing in the wide segments. The flow and its pumping effect have been studied numerically as well as experimentally. In practical applications, however, a large number of segments should be used, so that the estimate of the properties and performance of the compressor in various steady and unsteady situations by the DSMC computation or by experiment is a formidable task. Therefore, the simple macroscopic system summarized in Sec. 3 is useful for this purpose.

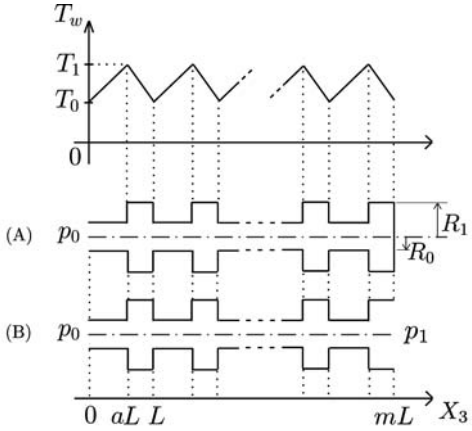

Fig. 6. – Knudsen compressor consisting of circular tubes.

Let us consider the system shown in Fig. 6, that is, a pipe composed of alternately arranged m narrow circular tubes (radius R_0 and length aL) and m wide circular tubes [radius R_1 and length $(1-a)L$], set in the interval $0 \le X_3 \le mL$. The temperature $T_w(X_3)$ of the pipe wall has a saw-tooth shape as

shown in the figure, i.e.,

$$(42)\quad T_w = \begin{cases} T_0, & \text{at } X_3 = nL \text{ and } mL, \\ T_1, & \text{at } X_3 = (a+n)L, \end{cases} \qquad (n = 0, 1, 2, \ldots, m-1),$$

and $T_w(X_3)$ is a piecewise linear function of X_3 joining T_0 and T_1. We assume that the assumptions (i)–(iii) of Sec. 3 are satisfied, so that (iv) there is also fulfilled. We consider the following two situations (Fig. 6):

(A) The pipe is closed at $X_3 = mL$, and the pressure at the open end $X_3 = 0$ is kept at p_0.

(B) Both ends are open, and the pressure at $X_3 = 0$ and that at $X_3 = mL$ are kept at p_0 and p_1, respectively.

We take p_0, T_0, R_0, and L as the reference quantities p_*, T_*, R_*, and L_*, respectively. Therefore, $\hat{T}_w(z) = 1$ at $z = n$ $(n = 0, 1, 2, \ldots, m-1)$ and m, and $\hat{T}_w(z) = T_1/T_0$ at $z = a + n$, and K_* is the Knudsen number of the inlet condition. In addition, the end conditions become

$$(43a)\quad \hat{p}_{(0)} = 1 \ (\text{at } z = 0), \quad M_{(1)} = 0 \ (\text{at } z = m) \quad \text{in Case (A)},$$

$$(43b)\quad \hat{p}_{(0)} = 1 \ (\text{at } z = 0), \quad \hat{p}_{(0)} = p_1/p_0 \ (\text{at } z = m) \quad \text{in Case (B)}.$$

We solve Eq. (34) with end conditions (43) and the initial condition

$$(44)\qquad \hat{p}_{(0)} = 1, \quad \text{at } \hat{t} = 0, \ \text{for } 0 < z < 1,$$

and obtain the steady solution as the long-time limit of the unsteady solution. In the final steady state, $M^i_{(1)} = 0$ in case (A), and $M^i_{(1)} \equiv M_f = \text{const.}$ in case (B). In the latter case, the mass-flow rate $\mathcal{M}$ is given by [cf. Eq. (39b)]

$$(45)\qquad \mathcal{M} = \pi\rho_0(2\mathcal{R}T_0)^{1/2}R_0^2\,[M_f\varepsilon + O(\varepsilon^2)],$$

where $\rho_0 = p_0/\mathcal{R}T_0$ and $\varepsilon = R_0/L$.

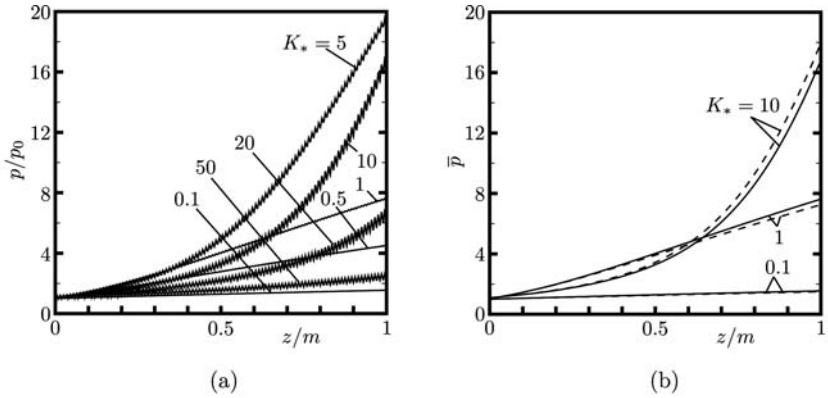

Fig. 7. – Steady pressure distribution along the pipe in Case (A) for $R_1/R_0 = 2$, $a = 0.5$, $T_1/T_0 = 1.5$, and $m = 100$ (N_2 gas: Pr $= 0.787$ and $\mu_b/\mu = 0.722$). (a) Various K_*, (b) Average pressure distribution for N_2 gas and monatomic gas (Pr $= 2/3$). In (b), the solid lines indicate the results for N_2 gas, and the dashed lines those for a monatomic gas.

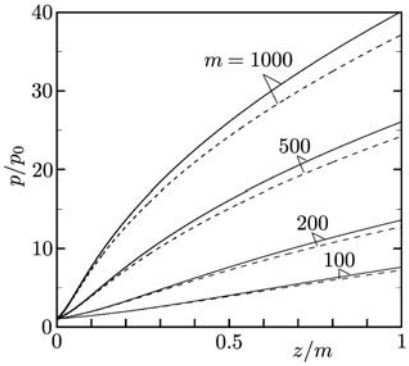

Fig. 8. – Steady pressure distribution along the pipe in Case (A) for $K_* = 1$, $T_1/T_0 = 1.5$, $a = 0.5$, and $R_1/R_0 = 2$. Various m for the N_2 gas and monatomic gas. The solid lines indicate the results for the N_2 gas, and the dashed lines those for the monatomic gas.

Some numerical results for the steady pressure distribution along the pipe, i.e., p/p_0 versus z, in case (A) are shown in Figs. 7 and 8 for N_2 gas ($\mathrm{Pr} = 0.787$ and $\mu_b/\mu = 0.722$). Figure 7 shows p/p_0 versus z for $m = 100$ in the case of $R_1/R_0 = 2$, $a = 0.5$, and $T_1/T_0 = 1.5$: Fig. 7(a) shows the effect of different K_*, and Fig. 7(b) the comparison between N_2 gas and a monatomic gas ($\mathrm{Pr} = 2/3$) for $K_* = 0.1$, 1, and 10. In the latter figure, we show the average pressure $\overline{p}$ over each segment, rather than the pressure p itself, to make the difference clearer. A relatively high pressure rise at the closed end can be obtained for intermediate values of the entrance Knudsen number [Fig. 7(a)]. The pressure distribution for large numbers of the segments (i.e., large m) is shown in Fig. 8 for $R_1/R_0 = 2$, $a = 0.5$, $T_1/T_0 = 1.5$, and $K_* = 1$. In the case of $m = 1000$, the pressure at the closed end for N_2 gas becomes about 40 times the pressure at the open end.

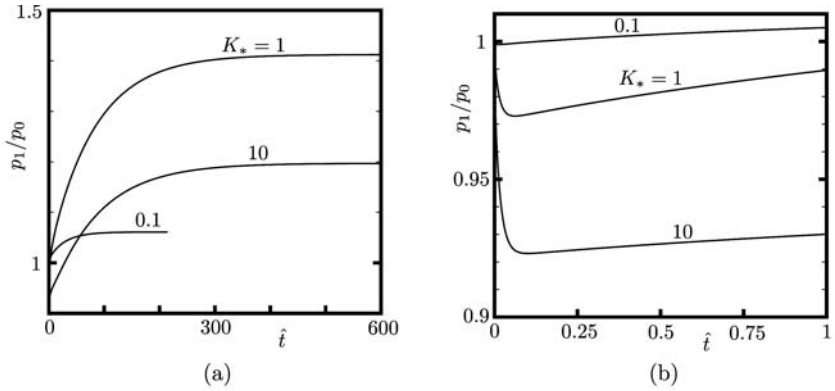

Fig. 9. – Time evolution of the pressure p_1 at the closed end ($X_3 = mL$) in Case (A) for $m = 10, T_1/T_0 = 1.5$, $a = 0.5$, and $R_1/R_0 = 2$. (a) $0 \le \hat{t} \le 600$, (b) $0 \le \hat{t} \le 1$.

An example of the manner of approach of the gas to the final steady state in Case (A) is shown in Fig. 9 for N_2 gas. More precisely, the time evolution of the pressure p_1 at the closed end ($z = m$ or $X_3 = mL$) versus $\hat{t}$ is plotted for $m = 10$ in the case of $R_1/R_0 = 2$, $a = 0.5$, and $T_1/T_0 = 1.5$. Figure 9(a) shows the global behavior ($0 \leq \hat{t} \leq 600$), and Fig. 9(b) the short-time behavior ($0 \leq \hat{t} \leq 1$). The approach is slower for intermediate and large Knudsen numbers ($K_* = 1$ and 10).

Finally, we show in Table 3 the steady mass-flow rate M_f [Eq. (45)] in case (B) for different m and K_* in the case of $R_1/R_0 = 2$, $a = 0.5$, $T_1/T_0 = 1.5$, $p_1/p_0 = 2$, and $K_* = 1$. The results for N_2 (Pr = 0.787 and $\mu_b/\mu = 0.722$) as well as for a monatomic gas (Pr = 2/3) are shown in the table. For small Knudsen numbers ($K_* = 0.1$), the flow from the high-pressure end to the low-pressure end dominates (i.e., M_f is negative) even for $m = 200$. However, for intermediate and large Knudsen numbers ($K_* = 1$ and 10), the flow induced by the wall-temperature distribution overcomes the pressure-driven flow (i.e., M_f is positive).

TABLE 3. – Steady mass-flow rates M_f versus the number of the units m in Case (B).

	$M_f\|_{\mathrm{Pr}=2/3}$			$M_f\|_{\mathrm{Pr}=0.787}$		
m	$K_* = 10$	$K_* = 1$	$K_* = 0.1$	$K_* = 10$	$K_* = 1$	$K_* = 0.1$
10	−8.080(− 2)*	−7.037(− 2)	−4.451(− 1)	−8.161(− 2)	−6.667(− 2)	−3.875(− 1)
50	1.096(− 2)	3.382(− 2)	−7.268(− 2)	9.971(− 3)	3.279(− 2)	−6.127(− 2)
100	1.935(− 2)	4.286(− 2)	−2.612(− 2)	1.851(− 2)	4.133(− 2)	−2.049(− 2)
200	2.127(− 2)	4.439(− 2)	−2.842(− 3)	2.055(− 2)	4.275(− 2)	−1.082(− 4)

* Read as -8.080×10^{-2}

5. – Concluding remarks.

In the present study, we considered two fundamental and classical problems of rarefied gas dynamics, Poiseuille flow and thermal transpiration through a circular tube for a polyatomic gas. Our basic equation is the linearized version of the ES model of the Boltzmann equation for a polyatomic gas. But, we showed that the solution of the thermal transpiration through a circular tube based on the ES model for a polyatomic gas is identical with that based on the BGK model for a monatomic gas, and that the solution of the Poiseuille flow through a circular tube based on the ES model for a polyatomic gas is obtained by a simple conversion formula from that based on the BGK model for a monatomic gas. Therefore, we were able to obtain the profiles of the flow velocity and heat flow as well as the mass-flow rate for the present problem, exploiting the existing database for the BGK model for a monatomic gas (Sec. 2).

On the other hand, we derived a macroscopic equation of diffusion type and the connection conditions that describe the pressure distribution in a pipe consisting of many thin circular tubes with different radii connected one after another. The resulting macroscopic system is summarized in Sec. 3. With the database for the mass-flow rates mentioned above, the macroscopic system became applicable to practical problems of microscale gas flows when the pipe consists of circular tubes and the behavior of the gas is described by the ES model for a polyatomic gas.

Finally, we applied the macroscopic system to a gas flow through a single long circular tube caused by a large pressure difference imposed at both ends (Sec. 4.1) and to a Knudsen compressor consisting of many alternately arranged thinner and thicker circular tubes (Sec. 4.2). With this procedure, we were able to obtain the pressure distribution along the pipe and the mass-flow rate through the pipe in the two problems easily.

It should be stressed that the direct numerical analysis of such problems, either by the DSMC method or by finite-difference methods based on the model Boltzmann equations, is a formidable task. Therefore, the present approach, using the diffusion-type system plus the database for the Poiseuille-flow and thermal-transpiration mass-flow rates, provides a useful and powerful tool. The applicability of the diffusion-type system can be extended easily just by constructing the corresponding database for the tubes with different cross sections.

Acknowledgments. K. A. wishes to express his heartfelt thanks to Carlo Cercignani for his guidance, collaboration, and friendship over the last three decades. This work was supported by the grant-in-aid for scientific research No. 20360046 from JSPS.

Appendix A ES model of the Boltzmann equation.

In this appendix, we summarize the ES model of the Boltzmann equation for a polyatomic gas. Let us consider a gas consisting of molecules with internal degree of freedom δ. The number of the molecules with position in d^3X around $\boldsymbol{X}$, velocity in $d^3\xi$ around $\boldsymbol{\xi}$, and energy related to the internal degree of freedom in $d\widetilde{\mathcal{E}}$ around $\widetilde{\mathcal{E}}$ at time t is written as

$$\frac{1}{m} f(t, \boldsymbol{X}, \boldsymbol{\xi}, \widetilde{\mathcal{E}}) d^3X d^3\xi d\widetilde{\mathcal{E}}, \tag{46}$$

where f is the velocity and energy distribution function of the gas molecules, and m is the mass of a molecule. The ES model for a polyatomic gas can be written in the following form [1] (see the last paragraph of this appendix for the difference

in notations between Ref. [1] and the present paper):

$$\frac{\partial f}{\partial t} + \xi_j \frac{\partial f}{\partial X_j} = A_c(T)\rho(\mathcal{G}[f] - f), \tag{47a}$$

$$\mathcal{G}[f] = \frac{\rho \Lambda_\delta \widetilde{\mathcal{E}}^{\delta/2-1}}{(2\pi)^{3/2}|\underline{\mathcal{I}}|^{1/2}(\mathcal{R}T_{\mathrm{rel}})^{\delta/2}} \times \exp\Big(-\frac{1}{2}{}^t(\boldsymbol{\xi}-\boldsymbol{v})\cdot\underline{\mathcal{I}}^{-1}\cdot(\boldsymbol{\xi}-\boldsymbol{v}) - \frac{\widetilde{\mathcal{E}}}{\mathcal{R}T_{\mathrm{rel}}}\Big), \tag{47b}$$

$$\underline{\mathcal{I}} = (1-\eta)\Big[(1-\nu)\mathcal{R}T_{\mathrm{tr}}\underline{Id} + \nu\underline{\Theta}\Big] + \eta\mathcal{R}T\underline{Id}, \tag{47c}$$

$$\underline{\Theta} = \frac{1}{\rho}\iint_0^\infty (\boldsymbol{\xi}-\boldsymbol{v})\cdot{}^t(\boldsymbol{\xi}-\boldsymbol{v}) f d\widetilde{\mathcal{E}} d^3\xi, \tag{47d}$$

$$\rho = \iint_0^\infty f d\widetilde{\mathcal{E}} d^3\xi, \tag{47e}$$

$$v_i = \frac{1}{\rho}\iint_0^\infty \xi_i f d\widetilde{\mathcal{E}} d^3\xi, \tag{47f}$$

$$T_{\mathrm{tr}} = \frac{1}{3\rho\mathcal{R}}\iint_0^\infty (\xi_i - v_i)^2 f d\widetilde{\mathcal{E}} d^3\xi, \tag{47g}$$

$$T_{\mathrm{int}} = \frac{2}{\delta\rho\mathcal{R}}\iint_0^\infty \widetilde{\mathcal{E}} f d\widetilde{\mathcal{E}} d^3\xi, \tag{47h}$$

$$T = \frac{3T_{\mathrm{tr}} + \delta T_{\mathrm{int}}}{3+\delta}, \tag{47i}$$

$$T_{\mathrm{rel}} = \eta T + (1-\eta)T_{\mathrm{int}}. \tag{47j}$$

Here, ρ is the mass density of the gas, v_i is the flow velocity, T is the temperature, T_{tr} is the temperature related to the translational energy, T_{int} is the temperature related to the energy of the internal degree of freedom, and $\mathcal{R}$ is the specific gas constant (the Boltzmann constant divided by the mass of a molecule); $\nu \in [-1/2, 1)$ and $\eta \in (0, 1]$ are the parameters to adjust the Prandtl number and the bulk viscosity to the gas under consideration [see Eqs. (51c) and (51d)]; $A_c(T)$ is a function of T such that $A_c(T)\rho$ is the collision frequency of the gas molecules, and Λ_δ is a dimensionless constant defined by

$$\Lambda_\delta^{-1} = \int_0^\infty s^{\delta/2-1}e^{-s}ds. \tag{48}$$

In addition, $\underline{\mathcal{T}}$ and $\underline{\Theta}$ are 3×3 symmetric matrices, $\underline{Id}$ is the 3×3 identity matrix, $|\underline{\mathcal{T}}|$ and $\underline{\mathcal{T}}^{-1}$ are the determinant and the inverse matrix of $\underline{\mathcal{T}}$, respectively, and the symbol ^{t} indicates the transpose operation. In what follows, for an arbitrary matrix $\underline{A}$, its (i, j) component, determinant, inverse matrix, and transposed matrix are denoted by A_{ij}, $|\underline{A}|$, $\underline{A}^{-1}$, and ${}^t\underline{A}$, respectively. In the above equations, $d^3\xi = d\xi_1 d\xi_2 d\xi_3$, and the domain of integration with respect to ξ_i is the whole space of ξ_i. It should be noted that the pressure p and the stress tensor p_{ij} are given by

$$p = \rho \mathcal{R} T, \tag{49a}$$

$$p_{ij} = \rho \Theta_{ij} = \iint_0^\infty (\xi_i - v_i)(\xi_j - v_j) f d\widetilde{\mathcal{E}} d^3\xi. \tag{49b}$$

The vanishing right-hand side of Eq. (47a) is equivalent to the fact that f is a local equilibrium distribution f_{eq} [1]:

$$f_{\mathrm{eq}} = \frac{\rho \Lambda_\delta}{(2\pi\mathcal{R}T)^{3/2}(\mathcal{R}T)^{\delta/2}} \widetilde{\mathcal{E}}^{\delta/2-1} \exp\Big(-\frac{(\xi_i - v_i)^2}{2\mathcal{R}T} - \frac{\widetilde{\mathcal{E}}}{\mathcal{R}T}\Big). \tag{50}$$

It is also known [1] that Eq. (47) leads to the viscosity μ, the thermal conductivity κ, the Prandtl number Pr, and the bulk viscosity μ_b in the following form:

$$\mu = \frac{1}{1 - \nu + \eta\nu} \frac{\mathcal{R}T}{A_c(T)}, \tag{51a}$$

$$\kappa = \frac{\gamma}{\gamma - 1} \mathcal{R} \frac{\mathcal{R}T}{A_c(T)}, \tag{51b}$$

$$\mathrm{Pr} = \frac{\gamma}{\gamma - 1} \frac{\mathcal{R}\mu}{\kappa} = \frac{1}{1 - \nu + \eta\nu}, \tag{51c}$$

$$\mu_b = \frac{1}{\eta}\Big(\frac{5}{3} - \gamma\Big) \frac{\mu}{\mathrm{Pr}}, \tag{51d}$$

with γ the ratio of the specific heats given by

$$\gamma = \frac{\delta + 5}{\delta + 3}. \tag{52}$$

Equation (47) contains the set of parameters (ν, η, δ) characterizing the gas under consideration. In place of this set, we may use another set $(\mathrm{Pr}, \mu_b/\mu, \delta)$ because of relations (51c), (51d), and (52).

The molecular mean free path l_0 in an equilibrium state at rest at tempera-

ture T_0 and density ρ_0 is defined as

$$l_0 = \frac{2}{\sqrt{\pi}} \frac{(2\mathcal{R}T_0)^{1/2}}{A_c(T_0)\rho_0}, \tag{53}$$

in terms of the mean molecular speed $(2/\sqrt{\pi})(2\mathcal{R}T_0)^{1/2}$ and the collision frequency $A_c(T_0)\rho_0$ in the equilibrium state. Therefore, the viscosity μ_0, the thermal conductivity κ_0, and the bulk viscosity μ_{b0} corresponding to the equilibrium state are expressed (in terms of l_0) as

$$\mu_0 = \frac{\sqrt{\pi}}{2} \frac{1}{1-\nu+\eta\nu} \frac{p_0}{(2\mathcal{R}T_0)^{1/2}} l_0, \tag{54a}$$

$$\kappa_0 = \frac{\sqrt{\pi}}{2} \frac{\gamma}{\gamma-1} \frac{\mathcal{R}p_0}{(2\mathcal{R}T_0)^{1/2}} l_0, \tag{54b}$$

$$\mu_{b0} = \frac{1}{\eta}\left(\frac{5}{3}-\gamma\right)\frac{\mu_0}{\mathrm{Pr}}. \tag{54c}$$

The diffuse-reflection condition [8, 9, 32], adapted to the present polyatomic case, on the boundary is expressed as

$$f = \frac{\rho_w \Lambda_\delta}{(2\pi\mathcal{R}T_w)^{3/2}(\mathcal{R}T_w)^{\delta/2}} \widetilde{\mathcal{E}}^{\delta/2-1} \exp\Big(-\frac{\xi_i^2}{2\mathcal{R}T_w} - \frac{\widetilde{\mathcal{E}}}{\mathcal{R}T_w}\Big), \quad (\boldsymbol{\xi}\cdot\boldsymbol{n} > 0), \tag{55a}$$

$$\rho_w = -\Big(\frac{2\pi}{\mathcal{R}T_w}\Big)^{1/2} \int_{\xi\cdot\boldsymbol{n}<0} \int_0^\infty \boldsymbol{\xi}\cdot\boldsymbol{n} f d\widetilde{\mathcal{E}} d^3\xi, \tag{55b}$$

where T_w is the temperature of the boundary, and $\boldsymbol{n}$ is the unit normal vector of the boundary pointed toward the gas.

In Ref. [1], the energy $\widetilde{\mathcal{E}}$, which is denoted by ε there, is assumed to be expressed as $\widetilde{\mathcal{E}} = I^{2/\delta}$ in terms of a variable I, and I is used as an independent variable. More specifically, the distribution function in Ref. [1], which we denote by $\overline{f}(t, \boldsymbol{X}, \boldsymbol{\xi}, I)$ here, is defined in such a way that

$$\frac{1}{m}\,\overline{f}(t, \boldsymbol{X}, \boldsymbol{\xi}, I) d^3X d^3\xi dI, \tag{56}$$

indicates the number of the molecules with position in d^3X around $\boldsymbol{X}$, velocity in $d^3\xi$ around $\boldsymbol{\xi}$, and the variable I in dI around I at time t. Therefore, the relation between $\overline{f}$ and the present f is as follows:

$$f(t, \boldsymbol{X}, \boldsymbol{\xi}, \widetilde{\mathcal{E}}) = (\delta/2)\widetilde{\mathcal{E}}^{\delta/2-1}\overline{f}(t, \boldsymbol{X}, \boldsymbol{\xi}, \widetilde{\mathcal{E}}^{\delta/2}). \tag{57}$$

In addition, Λ_δ in Ref. [1], which we denote by $\overline{\Lambda}_\delta$ here, is related to Λ_δ in Eq. (48) as

$$\Lambda_\delta^{-1} = (2/\delta)(\overline{\Lambda}_\delta)^{-1}. \tag{58}$$

REFERENCES

[1] P. Andries - P. Le Tallec - J.-P. Perlat - B. Perthame, *The Gaussian-BGK model of Boltzmann equation with small Prandtl number*, Eur. J. Mech. B/Fluids, **19** (2000), 813-830.

[2] K. Aoki - P. Degond, *Homogenization of a flow in a periodic channel of small section*, Multiscale Model. Simul., **1** (2003), 304-334.

[3] K. Aoki - P. Degond - L. Mieussens - M. Nishioka - S. Takata, *Numerical simulation of a Knudsen pump using the effect of curvature of the channel*, in *Rarefied Gas Dynamics*, M. S. Ivanov and A. K. Rebrov eds., Siberian Branch of the Russian Academy of Sciences, Novosibirsk, (2007), 1079-1084.

[4] K. Aoki - P. Degond - L. Mieussens - S. Takata - H. Yoshida, *A diffusion model for rarefied flows in curved channels*, Multiscale Model. Simul., **6** (2008), 1281-1316.

[5] K. Aoki - P. Degond - S. Takata - H. Yoshida, *Diffusion models for Knudsen compressors*, Phys. Fluids, **19** (2007), 117103.

[6] K. Aoki - S. Takata - K. Kugimoto, *Diffusion approximation for the Knudsen compressor composed of circular tubes*, in *Rarefied Gas Dynamics*, T. Abe ed., AIP, Melville, (2009), 953-958.

[7] P. L. Bhatnagar - E. P. Gross - M. Krook, *A model for collision processes in gases. I. Small amplitude processes in charged and neutral one-component systems*, Phys. Rev., **94** (1954), 511-525.

[8] C. Cercignani, *The Boltzmann Equation and Its Applications*, Springer-Verlag, Berlin (1988).

[9] C. Cercignani, *Rarefied Gas Dynamics, From Basic Concepts to Actual Calculations*, Cambridge Univ. Press, Cambridge (2000).

[10] C. Cercignani - A. Daneri, *Flow of a rarefied gas between two parallel plates*, J. Appl. Phys., **34** (1963), 3509-3513.

[11] C. Cercignani - F. Sernagiotto, *Cylindrical Poiseuille flow of a rarefied gas*, Phys. Fluids, **9** (1966), 40-44.

[12] C.-C. Chen - I.-K. Chen - T.-P. Liu - Y. Sone, *Thermal transpiration for the linearized Boltzmann equation*, Commn. Pure Appl. Math., **60** (2007), 0147-0163.

[13] P. Degond, *A model of near-wall conductivity and its application to plasma thrusters*, SIAM J. Applied Math., **58** (1998), 1138-1162.

[14] P. Degond - V. Latocha - L. Garrigues - J. P. Boeuf, *Electron transport in stationary plasma thrusters*, Transp. Theory and Stat. Phys., **27** (1998), 203-221.

[15] S. Fukui - R. Kaneko, *Analysis of ultra-thin gas film lubrication based on linearized Boltzmann equation including thermal creep flow*, J. Tribol., **110** (1988), 253-262.

[16] Y. L. Han - M. Young - E. P. Muntz - G. Shiflett, *Knudsen compressor performance at low pressures*, in *Rarefied Gas Dynamics*, M. Capitelli ed., AIP, Melville, (2005), 162-167.

[17] M. Hasegawa - Y. Sone, *Poiseuille and thermal transpiration flows of a rarefied gas for various pipes*, J. Vac. Soc. Jpn., **31** (1988), 416-419 (in Japanese).

[18] L. H. Holway, Jr., *Approximation procedures for kinetic theory*, Ph.D. Thesis, Harvard University (1963).
[19] L. H. Holway, Jr., *New statistical models for kinetic theory: Methods of construction*, Phys. Fluids, **9** (1966), 1658-1673.
[20] M. Knudsen, *Eine Revision der Gleichgewichtsbedingung der Gase. Thermische Molekularströmung*, Ann. Phys., **31** (1910), 205-229.
[21] M. Knudsen, *Thermischer Molekulardruck der Gase in Röhren*, Ann. Phys., **33** (1910), 1435-1448.
[22] S. K. Loyalka, *Thermal transpiration in a cylindrical tube*, Phys. Fluids, **12** (1969), 2301-2305.
[23] S. K. Loyalka - T. S. Storvick - H. S. Park, *Poiseuille flow and thermal creep flow in long, rectangular channels in the molecular and transition flow regimes*, J. Vac. Sci. Technol., **13** (1976), 1188-1192.
[24] L. Marino, *Experiments on rarefied gas flows through tubes*, Microfluid Nanofluid, **6** (2009), 109-119.
[25] National Institutes of Natural Sciences and National Astronomical Observatory of Japan (eds.), *Chronological Scientific Tables*, Maruzen, Tokyo, (1994) (in Japanese).
[26] H. Niimi, *Thermal creep flow of rarefied gas between two parallel plates*, J. Phys. Soc. Jpn., **30** (1971), 572-574.
[27] T. Ohwada - Y. Sone - K. Aoki, *Numerical analysis of the Poiseuille and thermal transpiration flows between two parallel plates on the basis of the Boltzmann equation for hard-sphere molecules*, Phys. Fluids A, **1** (1989), 2042-2049.
[28] G. J. Prangsma - A. H. Alberga - J. J. M. Beenakker, *Ultrasonic determination of the volume viscosity of* N_2, CO, CH_4 *and* CD_4 *between 77 and 300 K*, Physica, **64** (1973), 278-288.
[29] F. Sharipov - G. Bertoldo, *Poiseuille flow and thermal creep based on the Boltzmann equation with the Lennard-Jones potential over a wide range of the Knudsen number*, Phys. Fluids, **21** (2009), 067101.
[30] F. Sharipov - V. Seleznev, *Data on internal rarefied gas flows*, J. Phys. Chem. Ref. Data, **27** (1998), 657-706.
[31] C. E. Siewert, *The linearized Boltzmann equation: Concise and accurate solutions to basic flow problems*, Z. angew. Math. Phys., **54** (2003), 273-303.
[32] Y. Sone, *Molecular Gas Dynamics: Theory, Techniques, and Applications*, Birkhäuser, Boston (2007).
[33] Y. Sone - E. Itakura, *Analysis of Poiseuille and thermal transpiration flows for arbitrary Knudsen numbers by a modified Knudsen number expansion and their database*, J. Vac. Soc. Jpn., **33** (1990), 92-94 (in Japanese).
[34] Y. Sone - K. Sato, *Demonstration of a one-way flow of a rarefied gas induced through a pipe without average pressure and temperature gradients*, Phys. Fluids, **12** (2000), 1864-1868.
[35] Y. Sone - H. Sugimoto, *Vacuum pump without a moving part and its performance*, in *Rarefied Gas Dynamics*, A. Ketsdever and E. P. Muntz eds., AIP, Melville, (2003), 1041-1048.
[36] Y. Sone - Y. Waniguchi - K. Aoki, *One-way flow of a rarefied gas induced in a channel with a periodic temperature distribution*, Phys. Fluids, **8** (1996), 2227-2235.
[37] Y. Sone - K. Yamamoto, *Flow of rarefied gas through a circular pipe*, Phys. Fluids, **11** (1968), 1672-1678.
[38] H. Sugimoto - Y. Sone, *Vacuum pump without a moving part driven by thermal edge flow*, in *Rarefied Gas Dynamics*, M. Capitelli ed., AIP, Melville, (2005), 168-173.

[39] S. TAKATA - H. FUNAGANE - K. AOKI, *Fluid modeling for the Knudsen compressor: Case of polyatomic gases*, Kinetic and Related Models, **3** (2010), 353-372.
[40] S. TAKATA - H. SUGIMOTO - S. KOSUGE, *Gas separation by means of the Knudsen compressor*, Eur. J. Mech. B/Fluids, **26** (2007), 155-181.
[41] S. E. VARGO - E. P. MUNTZ, *An evaluation of a multiple-stage micromechanical Knudsen compressor and vacuum pump*, in *Rarefied Gas Dynamics*, C. Shen ed., Peking University Press, Peking, (1997), 995-1000.
[42] P. WELANDER, *On the temperature jump in a rarefied gas*, Ark. Fys., **7** (1954), 507-553.

Hitoshi Funagane: Department of Mechanical Engineering and Science,
Kyoto University, Kyoto 606-8501, Japan
E-mail: f.hitoshi@at8.ecs.kyoto-u.ac.jp

Shigeru Takata: Department of Mechanical Engineering and Science,
Kyoto University, Kyoto 606-8501, Japan
E-mail: takata@aero.mbox.media.kyoto-u.ac.jp

Kazuo Aoki: Department of Mechanical Engineering and Science,
Kyoto University, Kyoto 606-8501, Japan
E-mail: aoki@aero.mbox.media.kyoto-u.ac.jp

Ko Kugimoto: Department of Mechanical Engineering and Science,
Kyoto University, Kyoto 606-8501, Japan

Received July 22, 2010 and in revised form November 1, 2010